Plasma Processes and Polymers

PLASMA PROCESSES AND POLYMERS

BRIEF COMMUNICATION OPEN ACCESS

Investigation of a Hybrid Discharge Mode of a Pin-to-Plate DBD in Ar-Hexamethyldisilane and Its Influence on Thin Film Deposition

Lars Bröcker[1] | Claus-Peter Klages[1] | Markus M. Becker[2] | Detlef Loffhagen[2] | Marjan Stankov[2]

[1]Institute for Surface Technology, Technische Universität Braunschweig, Braunschweig, Germany | [2]Leibniz Institute for Plasma Science and Technology, Greifswald, Germany

Correspondence: Lars Bröcker (l.broecker@tu-braunschweig.de)

Received: 17 February 2025 | **Revised:** 16 April 2025 | **Accepted:** 5 May 2025

Funding: The work has been funded by the Deutsche Forschungsgemeinschaft (DFG, German Research Foundation)—project number 504701852.

Keywords: argon | dielectric barrier discharge | growth hillocks | hexamethyldisilane | hybrid mode

ABSTRACT

The study reports on a hybrid discharge mode found by experiment and modelling in a pin-to-plate atmospheric-pressure dielectric-barrier discharge using argon with small admixtures of hexamethyldisilane (HMDS). Optical observations in the early stages of discharge operation reveal a unique discharge structure with a diffusive part and a strongly contracted, bright region in front of the grounded substrate. To investigate the observed discharge characteristics, fluid modelling of the plasma evolution during the ignition phase is performed. Modelling results reproduce the discharge behaviour, uncover the discharge dynamics, and reveal the role of relevant plasma-chemical processes. Surfaces of films deposited in the hybrid mode are covered by flat hillocks indicating a close relationship to filaments observed with the bare eye and in modelling.

1 | Introduction

In the search for efficient plasma-enhanced chemical vapour deposition (PECVD) processes, different plasma phenomena have been observed using various configurations of dielectric-barrier discharge (DBD) sources operating under different conditions [1]. This manuscript reports on the specific discharge appearance observed in an atmospheric-pressure DBD in Ar with small admixtures of organosilicon monomers and its impact on film deposition.

Atmospheric-pressure DBDs can operate in different diffuse modes (e.g., atmospheric-pressure Townsend discharge [APTD], atmospheric-pressure glow discharge [APGD]) or in filamentary modes, depending on the working conditions [2–4]. Additionally, a wide range of intermediate or hybrid modes of operation is also possible. Boisvert et al. [5] for example, reports on a hybrid discharge mode found in a helium DBD at atmospheric pressure in an intermediate frequency range where the transition from APGD to RF-α (radio-frequency-α) mode takes place, exhibiting properties from both. In Höft et al. [6] a study on a sinusoidal-operated DBD in N_2 with admixtures of N_2O led to the identification of another hybrid discharge mode described as an alternating APTD and filamentary discharge, depending on the sign of the applied voltage. A key point is that plasma exhibits distinct properties in each discharge mode, with some modes proving highly advantageous for specific applications while being entirely unsuitable for others.

In PECVD using atmospheric-pressure DBDs, all of the above-mentioned discharge modes can occur with varying effects on the deposited film quality. For example, homogeneous modes provide excellent uniformity [7]. Films deposited in filamentary mode often show poor uniformity due to localised plasma channels, causing over-processing in some areas and insufficient treatment in others [8]. Reasonable uniformity can be achieved with hybrid or intermediate modes at lower power and

current densities limiting film penetration [2]. To ensure optimal PECVD performance the discharge mode of the plasma source has to be identified and well understood.

In this study, a hybrid discharge regime is presented that is not comparable to any of the plasma modes reported so far. More specifically, a unique discharge with a clearly formed diffusive region and, for the first few seconds, a strongly contracted, bright spot with a diameter of approximately 100 µm was optically observed in a pin-to-plate DBD setup with pin-backed glass dielectric facing an electrically conductive plate. Afterwards, stochastically moving, thin discharge channels appear between the diffuse plasma region and the grounded silicon substrate. The term 'hybrid' refers therefore to a regime, where a diffuse and filamentary part occurs at the same time but in different regions of the discharge gap.

The reported discharge behaviour was achieved in argon at atmospheric pressure with small fractions ($x_M \leq 200$ ppm) of an organosilicon monomer for comparatively short deposition times $t_d < 120$ s. To uncover the mechanism of hybrid regime formation, the electrical characteristics of the discharge were analysed and time-dependent, spatially two-dimensional (2d-t) fluid-Poisson discharge modelling for a mixture of argon and 100 ppm hexamethyldisilane (HMDS, $(CH_3)_3SiSi(CH_3)_3$) was employed. Additionally, the influence of the discharge on the film formation was investigated by laser-scanning microscopy (LSM) for HMDS fractions of 25 and 50 ppm and $t_d = 60$ s.

2 | Methods

2.1 | Experimental Setup and Diagnostics

The used setup consists of a manually sharpened pin (tungsten, 1.6 mm diameter, 35 mm length, tip angle 23°) glued onto a 1.1-mm thick borosilicate glass as the high voltage electrode and a grounded aluminium bottom carrying an ethanol-cleaned silicon wafer piece (10 mm × 22 mm) as substrate for film deposition. Experiments were performed with mixtures of argon (6.0 purity, Linde AG) and HMDS (purity of 97%, abcr GmbH) flowing with an average velocity of 50 cm/s through the 2.5-mm gap between substrate surface and dielectric. The DBDs were driven by a sinusoidal voltage (amplitude $U_{a0} = 1.75$ kV, frequency $f = 19$ kHz). A schematic diagram is shown in Figure 1, a detailed description can be found in references [9] and [10].

Snapshots were taken from a video, see also [11], for $x_M = 100$ ppm using a Canon EOS 7D Mark II camera at 25 frames/s and brightened by 40%. Micrographs and topography information of deposits for $x_M = 25$ and 50 ppm, respectively, were obtained by LSM (Keyence Deutschland GmbH, VK-X3000) at magnifications of 5× and 150×, respectively. An oscilloscope (Tektronix MDO3052) was used to monitor the applied voltage $U_a(t)$ and the voltage drop $U_c(t)$ at a capacitor (1 nF) in series to the discharge setup to calculate the dissipated energy E_g and transferred charge Δq during one period from Lissajous figures. Current signals were obtained by replacing the capacitor by a 500 Ω resistor. The investigated monomer fraction was 50 ppm. For more details regarding the electrical characterisation, see [9] and [12]. For the measurement of the ignition voltage U_{Ig} for $x_M = 100$ ppm, U_{a0} was increased until the discharge was visible with the bare eye.

2.2 | Model Description

The DBD plasma source was modelled by means of a 2d-t fluid-Poisson model in cylindrical coordinates employing COMSOL Multiphysics [13] for the geometry sketched in Figure 1. The model considers balance equations for the species number densities and for the electron energy density. It also includes the Poisson equation for the electric potential calculations and a balance equation for the surface charge density accumulated at the dielectric surface. The balance equations were solved with appropriate boundary conditions according to [14, 15]. In particular, the applied voltage U_a was assigned to the pin electrode. Zero potential was set at the Si wafer surface, as its semiconductor properties result in much lower charge accumulation than dielectrics. Thus, it was treated as a metal in accordance with experimental insights. Initially, a spatially uniform distribution of species was assumed with a number density of 10^{12} m^{-3}

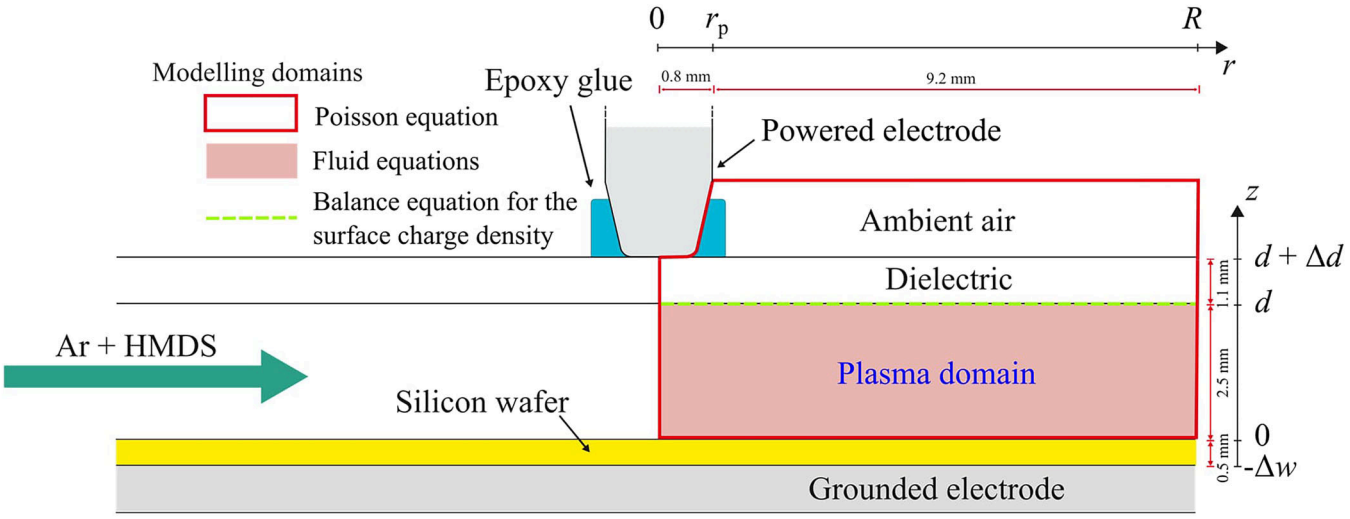

FIGURE 1 | Illustration of the investigated plasma source with annotated domains used in the modelling study.

for the excited and charged argon species and $10^6\,m^{-3}$ for the Si-containing ions. The initial electron number density was set to maintain quasi-neutrality. Details about the basic relations, modelling approach and the solution method are given in [16].

The reaction kinetic model (RKM) for the Ar-HMDS mixture takes into account argon-related and silicon-containing species as well as electrons. The argon part considers the ground state of the argon atom (Ar[$1p_0$]), three exited states of argon (Ar_m, Ar_r and Ar_p), two excited argon molecular states (Ar_2 [$^3\Sigma_u^+$, v = 0] and Ar_2 [$^1\Sigma_u^+$, v = 0]), as well as argon atomic (Ar^+) and molecular ion (Ar_2^+). The excited states Ar_m, Ar_r and Ar_p represent the two metastable $1s_{5,3}$, two resonant $1s_{4,2}$ and ten $2p_{10,\ldots,1}$ states, respectively. For silicon-containing species, the HMDS molecule and its ion as well as trimethylsilyl ($(CH_3)_3Si^+$) and pentamethyldisilan-1-yl ($(CH_3)_3SiSi^+(CH_3)_2$) ions are part of the RKM. The applied RKM involves about 60 collisional and radiative processes defined based on studies in [17, 18].

3 | Results and Discussion

Two phenomena found in DBDs with Ar-HMDS mixtures under the working conditions given in sub-section 2.1 are presented and discussed. The first phenomenon is related to the hybrid discharge appearance. The second one corresponds to the formation of a unique morphology of deposited films, characterised by a surface carrying a large density of flat hillocks.

3.1 | Discharge Appearance

Snapshots of the discharge for $x_M = 100$ ppm and $t_d < 1$ s, 40 s and 120 s are shown in Figure 2a–c, respectively. The first snapshot shows the initial formation of the hybrid mode with a diffuse part in the top 2 mm of the discharge gap and a strongly contracted, bright region with a diameter of approximately 100 µm in front of the Si wafer. After 10–20 s the plasma begins to broaden near the substrate and several thin discharge channels less than 100 µm wide can be seen with the naked eye moving quickly and seemingly randomly across the Si surface (Figure 2b). Due to the low frame rate (25 fps), snapshots suggest a homogeneous negative glow near the Si wafer but actually many 'dancing' filaments are emerging from the diffuse upper region, overlapping in the image.

In addition to HMDS, the hybrid mode described here was also observed in Penning mixtures of Ar with hexamethyldisiloxane, allyltrimethylsilane and tetramethylsilane, respectively. For higher x_M and/or larger t_d, the discharge appears as an APGD, as can be seen in Figure 2c. The plasma is less bright and stochastically moving filaments are absent. A video of the plasma appearance can be found in [11].

To support the observations mentioned in the text and in Figure 2, Figure 3a shows the discharge current I_d of the positive half wave for $t_d = 1$ s, 45 s and 300 s. The displacement current was subtracted. For all three deposition times, generally broad current peaks with a FWHM (full width at half maximum) between 0.4 and 0.6 µs are observed, which can be related to APGDs. Additionally, distinct features appearing as small and narrow peaks on top of the broad current signal can be seen when the hybrid mode is present: For $t_d = 1$ s two additional peaks are visible, while four or five appear for $t_d = 45$ s. In general, these small features differ in number (one to six) for different positive half waves measured between $0 \le t_d \le 100$ s. Interestingly, the FWHM of these additional peaks of approximately 40 ns is indicative of filaments, observed with the bare eye and shown as an erratically glowing, bright region in Figure 2b. It is worth to mention that for $t_d > 100$ s, where the discharge appears as an 'pure' APGD, the current peaks that are related to the appearance of filaments disappear completely. It is therefore unlikely that these peaks are related to noise. For increasing t_d, current peaks decrease in height (from 0.5 mA for $t_d = 1$ s to 0.3 mA for $t_d = 300$ s), which correlates with a decrease in the overall dissipated energy E_g in the plasma as well as the transferred charge Δq during one period in Figure 3b. E_g and Δq decline up to $t_d = 100$ s, which can be better seen for Δq as the values for E_g scatter more pronouncedly. After approximately 100 s, a plateau is reached. The beginning of the plateau region correlates with the time when the plasma reaches a 'stable state', namely an APGD. The lower brightness in Figure 2c can therefore be explained by a decrease of E_g as the thickness of the deposited plasma polymer increases.

To reveal the physical mechanisms leading to the occurrence of the observed hybrid mode, the modelling study follows the plasma evolution in a mixture of argon and 100 ppm HMDS from $t = 0$ ($U_a(t) = U_{a0}\sin(2\pi ft) = 0$) until the first breakdown event. Operating conditions from sub-section 2.1 were applied with the exception of U_{a0}. Here, a value of 3.5 kV was chosen to match the experimental determination of U_{Ig}.

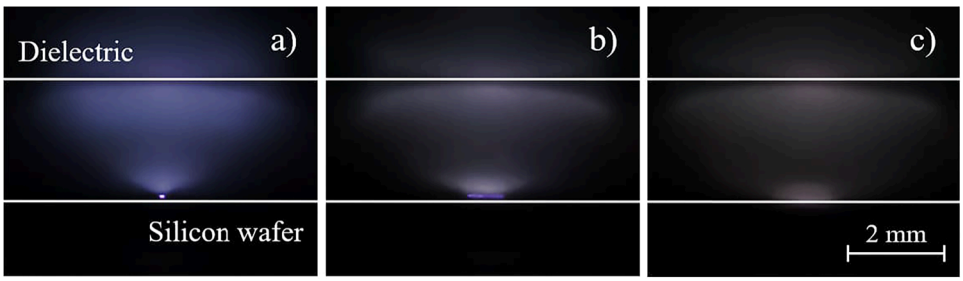

FIGURE 2 | Snapshots of the discharge formation for 100 ppm HMDS in argon showing the hybrid mode with (a) strongly contracted and bright region near the silicon wafer, $t_d < 1$ s, (b) erratically glowing and less bright region than in a), $t_d = 40$ s, see text for more information, and (c) an APGD, $t_d = 120$ s.

The analysis of the modelling results indicates that the plasma evolves through three discharge phases, as illustrated by representative spatial profiles of the electron number density n_e and the electric field magnitude $|E|$, shown for $t = 6$, 11 and 14.72 μs in Figure 4.

First, the Townsend pre-phase occurs as illustrated for $t = 6$ μs in Figure 4a,b. The results show the classical plasma behaviour in that phase, characterised by an increasing n_e in front of the anode and almost constant $|E|$.

With increasing $U_a(t)$, more charges are accumulated in the volume and a transient APGD discharge develops. It lasts from about $t = 7$ to 14 μs and is illustrated for $t = 11$ μs in Figure 4c,d. This phase is characterised by a diffusive quasi-neutral plasma region in front of the momentary anode ($z = d$), leading to small values of $|E|$ in that region. Here, the electron production comes mainly from Penning ionisation, that is, ionising collisions of excited argon species and HMDS. The quasi-neutral plasma region expands towards the momentary cathode ($z = 0$) with increasing time.

While $U_a(t)$ further increases, the plasma region spreads towards the momentary cathode and forms a momentary anode approaching the cathode. The electric field and electron density in the shrinking remainder of the gap becomes large enough to meet the conditions for inception of a positive streamer. This initiates the transition of the discharge from a diffuse APGD to the observed hybrid mode, which is characterised by a diffusive region in front of the anode (forming a virtual anode close to the momentary cathode) and a very thin and short plasma filament between the diffusive plasma region and the momentary cathode. In this phase, the high electron production results mainly from electron impact ionisation of argon atoms with the ionisation front moving at a velocity of about 10^5 m/s. Figure 4e,f illustrates the n_e and $|E|$ profiles as the streamer approaches the cathode at around $t = 14.72$ μs. The results reveal that n_e and $|E|$ in the streamer head reach values of approximately 10^{21} m^{-3}

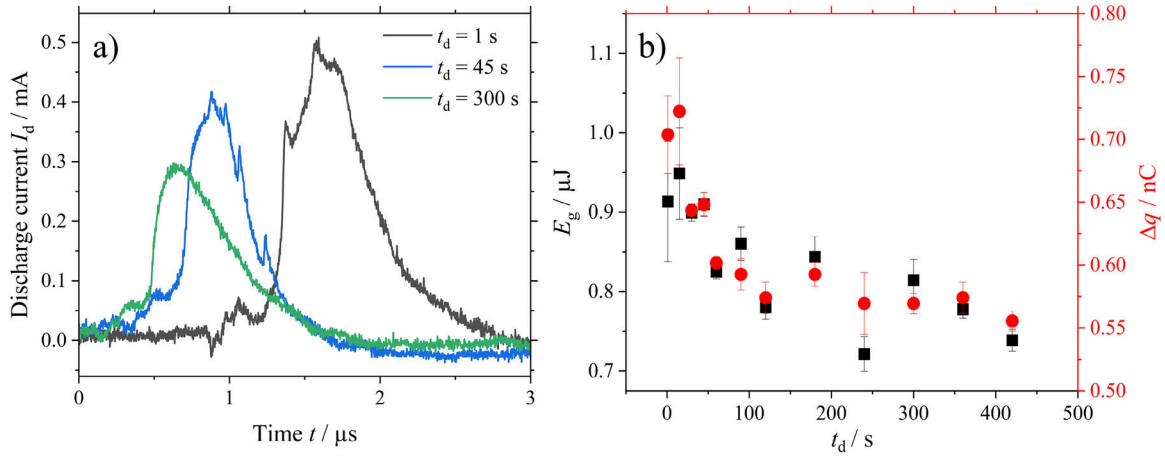

FIGURE 3 | (a) Discharge current I_d for $t_d = 1$ s (black line), 45 s (blue line) and 300 s (green line) and 50 ppm HMDS in Ar. The displacement current was subtracted. (b) Dissipated energy E_g and transferred charge Δq per period for the same monomer fraction x_M, calculated from Lissajous figures plotted against t_d.

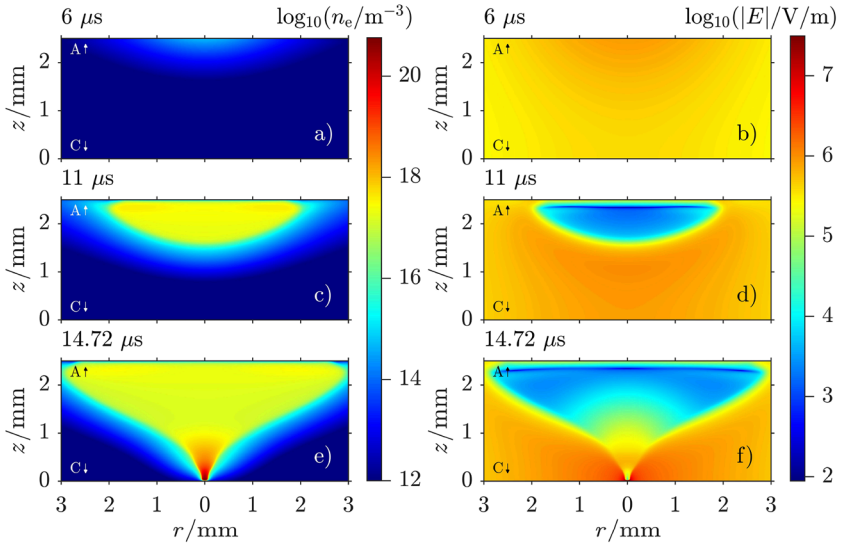

FIGURE 4 | Spatial profiles of n_e and |E| obtained by 2d-t modelling for (a, b) $t = 6$ μs, (c, d) $t = 11$ μs and (e, f) $t = 14.72$ μs for 100 ppm HMDS in argon. The momentary anode and cathode are marked with A and C, respectively.

and 10^7 V/m, respectively, in accordance with values for argon streamers [19]. It is important to emphasise that the n_e and |E| profiles in Figure 4e,f reflect the discharge pattern observed in the experiment demonstrating that this plasma behaviour is seemingly a consequence of the underlying plasma-chemical and -physical processes under the investigated conditions. Additionally, the modelling results for the second breakdown event, when the momentary cathode is at the opposite position ($z = 2.5$ mm), are not presented in this manuscript, since it is not the focus of this study. However, it should be mentioned that they do not predict the formation of a streamer, but a breakdown characteristic of an APGD. The maximum values of n_e and $|E|$ are approximately 10^{18} m^{-3} and 10^6 V/m, respectively, which is much lower than in the case of the streamer appearance shown in Figure 4e,f.

3.2 | Structure of Deposited Thin Films

A distinctive surface structure appears for the deposited plasma polymers from HMDS when the hybrid mode discussed in section 3.1 is present. Figure 5a shows a picture of a deposit made for 25 ppm HMDS admixture and after $t_d = 60$ s at 5× magnification. The deposit is overall bell-shaped with a diameter of approximately 1 mm where the film growth seems to be dot-wise. Black spots are penetrations through the film. The dot-wise film formation can even better be seen in Figure 5b,c for an HMDS fraction of 50 ppm and 150× magnification. Figure 5b) is acquired near the centre of the deposit and Figure 5c was recorded approximately 1 mm in gas flow direction from the centre. Changes in colours indicate different film thicknesses of the dots to the underlying plasma polymer film. Investigating the distribution of dots could uncover signs of cluster or line formations. A topography measurement from the section shown in Figure 5b reveals that the dots are in fact hillocks[1] with diameters between 1 and 10 µm and heights of 5–50 nm, see Figure 5d. From left to right the dots become higher in the direction of the centre.

It is reasonable to assume that filaments emerging from the homogeneous part of the plasma, visible in the video of the discharge appearance, current measurements (Figure 3a) as well as in the modelling (Figure 4) are related to the formation of the dot-wise plasma polymer deposition shown in Figure 5. Since every filament per positive half period is most likely responsible for the deposition of one dot, the discharge of the next period would be directed to a plasma-polymer-free location as a result of the electrically isolating character of the thin film. Another hypothesis, which

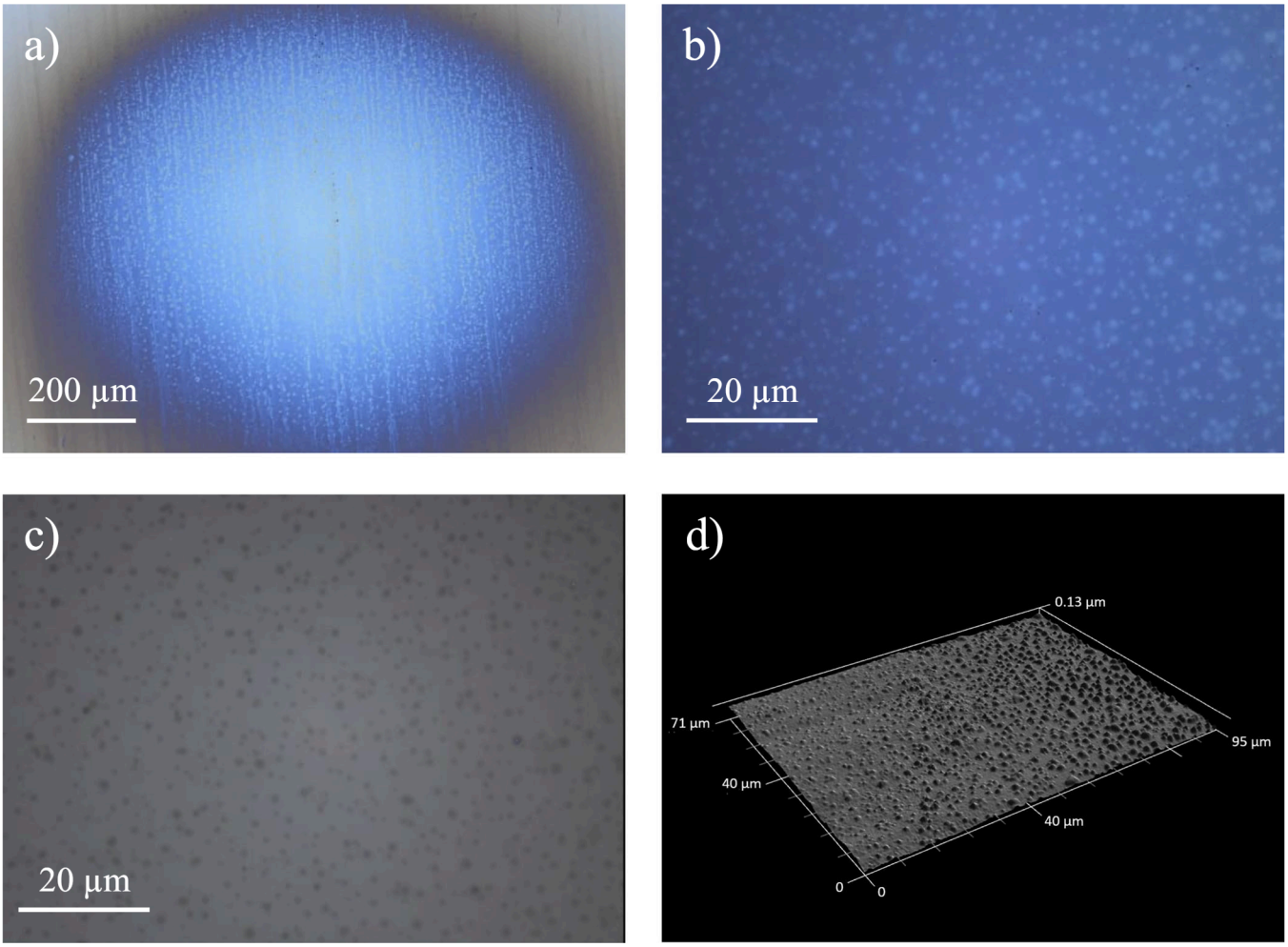

FIGURE 5 | Picture of a deposit for (a) 25 ppm HMDS, $t_d = 60$ s, magnification: 5× and (b) 50 ppm HMDS near the centre, $t_d = 60$ s, magnification: 150×. (c) Same deposit as for (b), but 1 mm away from the centre in gas flow direction. (d) Topography measurement of deposited area in (b).

correlates the dot-wise film deposition to an initial surface activation by observed filaments and a subsequent attachment of intact monomer molecules, is especially unlikely for HMDS and HMDSO due to the chemical nature of the precursors, since both monomers are not able to polymerise via a radical mechanism. After a continuous film of approximately 200 to 500 nm is deposited, the hybrid mode is not visible anymore and the discharge appears only as APGD (Figure 2c).[2] Future investigations will delve more into the formation mechanisms of the observed dot structures and their correlation to the different discharge modes. Here, scanning electron microscope images will be recorded to obtain an enhanced spatial resolution of the pictures in Figure 5.

4 | Summary

A hybrid discharge mode with a diffusive upper part and a contracted bright region in front of the grounded Si wafer is observed for small deposition times in a pin-to-plate atmospheric-pressure DBD, using argon with small admixtures of HMDS. 2d-t fluid modelling reveals that Penning ionisation leads to the ignition of a diffusive APGD, that spreads towards the cathode. It also shows that an increased electron density and electric field in the remainder of the gap initiates streamer inception which leads to the formation of a thin discharge channel between the diffusive region and the momentary cathode. Discharge currents indicate that several filaments per positive half wave can develop. LSM analysis of films deposited during this hybrid discharge shows a unique surface topography, characterised by a high density (roughly 10^7–10^8 cm^{-2}) of flat growth hillocks with heights and diameters of 5–50 nm and 1–10 µm, respectively. This finding leads to the hypothesis that the discharge filaments observed visually and by modelling are responsible for the unique surface topography and it potentially opens up new perspectives for optimising PECVD applications.

Acknowledgements

The work has been funded by the Deutsche Forschungsgemeinschaft (DFG, German Research Foundation)—project number 504701852. Open Access funding enabled and organized by Projekt DEAL.

Conflicts of Interest

The authors declare no conflicts of interest.

Data Availability Statement

The data that support the findings of this study are available from the corresponding author upon reasonable request.

Endnotes

[1] With this term, formed by adding the diminutive '-oc' to 'hill', the authors follow a long tradition in materials science to describe the small elevations that can form for varying reasons during film growth or—as negative features—during the etching of surfaces.

[2] It could be assumed that the inception of streamers to the substrate surface is related to the doping of the silicon wafer with boron and phosphorus but it is also observed with metal substrates like aluminium or stainless steel.

References

1. T. Belmonte, G. Henrion, and T. Gries, "Nonequilibrium Atmospheric Plasma Deposition," *Journal of Thermal Spray Technology* 20 (2011): 744–759.

2. F. Massines, C. Sarra-Bournet, F. Fanelli, N. Naudé, and N. Gherardi, "Atmospheric Pressure Low Temperature Direct Plasma Technology: Status and Challenges for Thin Film Deposition," *Plasma Processes and Polymers* 9 (2012): 1041–1073.

3. U. Kogelschatz, "Filamentary, Patterned, and Diffuse Barrier Discharges," *IEEE Transactions on Plasma Science* 30 (2002): 1400–1408.

4. R. Brandenburg, Z. Navrátil, J. Jánský, P. St'ahel, D. Trunec, and H.-E. Wagner, "The Transition Between Different Modes of Barrier Discharges at Atmospheric Pressure," *Journal of Physics D: Applied Physics* 42 (2009): 085208.

5. J.-S. Boisvert, J. Margot, and F. Massines, "Transitions of An Atmospheric-Pressure Diffuse Dielectric Barrier Discharge in Helium for Frequencies Increasing From kHz to MHz," *Plasma Sources Science and Technology* 26 (2017): 035004.

6. H. Höft, M. M. Becker, M. Kettlitz, et al., "Exploring the Mechanisms Leading to Diffuse and Filamentary Modes in Dielectric Barrier Discharges in N$$_2$$ With N$$_2$$O Admixtures," *European Physical Journal D* 77 (2023): 35.

7. P. A. Premkumar, S. A. Starostin, M. Creatore, et al., "Smooth and Self-Similar SiO_2-like Films on Polymers Synthesized in Roll-to-Roll Atmospheric Pressure-PECVD for Gas Diffusion Barrier Applications," *Plasma Processes and Polymers* 7 (2010): 635–639.

8. F. Massines and G. Gouda, "A Comparison of Polypropylene-Surface Treatment by Filamentary, Homogeneous and Glow Discharges in Helium at Atmospheric Pressure," *Journal of Physics D: Applied Physics* 31 (1998): 3411–3420.

9. L. Bröcker, G. S. Perlick, and C.-P. Klages, "Evidence of Ionic Film Deposition From Single-Filament Dielectric Barrier Discharges in Ar–HMDSO Mixtures," *Plasma Processes and Polymers (Print)* 17 (2020): 2000129.

10. L. Bröcker, T. Winzer, N. Steppan, J. Benedikt, and C.-P. Klages, "Plasma Polymerization of Allyltrimethylsilane With Single-Filament Dielectric-Barrier Discharges—Evidence of Cationic Surface Processes," *Plasma Processes and Polymers (Print)* 21 (2024): 2300177.

11. Supporting Information, https://www.tu-braunschweig.de/iot/institut/veroeffentlichungen/supporting-information (accessed: April 2025).

12. C.-P. Klages and L. Bröcker, "Induced and Transferred Charge in Dielectric-Barrier Discharge Setups Without 2D-Translational or Cylindrical Symmetry," *Plasma Processes and Polymers (Print)* 22 (2025): e70013.

13. COMSOL Multiphysics® v.6.2 COMSOL AB, Stockholm, Sweden, https://www.comsol.com/.

14. G. J. M. Hagelaar, F. J. de Hoog, and G. M. W. Kroesen, "Boundary Conditions in Fluid Models of Gas Discharges," *Physical Review E* 62 (2000): 1452–1454.

15. M. Stankov, M. M. Becker, R. Bansemer, K.-D. Weltmann, and D. Loffhagen, "Influence of Surface Parameters on Dielectric-Barrier Discharges in Argon at Subatmospheric Pressure," *Plasma Sources Science and Technology* 29 (2020): 125009.

16. A. P. Jovanovic, M. N. Stankov, D. Loffhagen, and M. M. Becker, "Automated Fluid Model Generation and Numerical Analysis of Dielectric Barrier Discharges Using Comsol," *IEEE Transactions on Plasma Science* 49 (2021): 3710–3718.

17. M. Stankov, M. M. Becker, T. Hoder, and D. Loffhagen, "Extended Reaction Kinetics Model for Non-Thermal Argon Plasmas and Its Test

Against Experimental Data," *Plasma Sources Science and Technology* 31 (2022): 125002.

18. D. Loffhagen, M. M. Becker, A. K. Czerny, and C.-P. Klages, "Modeling of Atmospheric-Pressure Dielectric Barrier Discharges in Argon With Small Admixtures of Tetramethylsilane," *Plasma Chemistry and Plasma Processing* 41 (2021): 289–334.

19. A. P. Jovanović, D. Loffhagen, and M. M. Becker, "Streamer–Surface Interaction in an Atmospheric Pressure Dielectric Barrier Discharge in Argon," *Plasma Sources Science and Technology* 31 (2022): 04LT02.